

## **Supporting Information**

# **Spatially Confined Single-Molecule Folding Achieves Multicolor Phosphorescence**

Xiaolu Zhou<sup>†</sup>, Xin-Kun Ma<sup>†</sup>, Xiaoye Zhang, Shuihuan Yu, Zhaoyuan Zhang and Yu Liu\*

College of Chemistry, State Key Laboratory of Elemento-Organic Chemistry, Nankai University,  
Tianjin 300071, P. R. China.

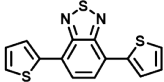
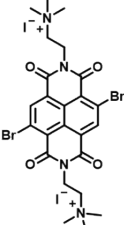
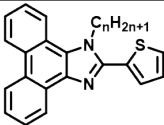
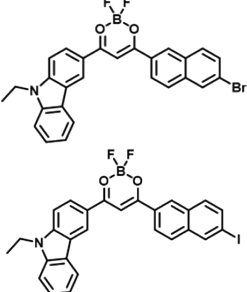
\*Corresponding author. Email: [yuliu@nankai.edu.cn](mailto:yuliu@nankai.edu.cn)

## 1. Materials and Measurements

All materials were purchased from commercialized suppliers and used as supplied unless otherwise noted. NMR spectra ( $^1\text{H}$  NMR and  $^{13}\text{C}$  NMR) were performed with an Ascend 400 MHz instrument. ROESY and COSY spectra were recorded on a ZhongKe-Oxford I-400 instrument. High-resolution mass spectrometry (HRMS) was given on a Q-TOF LC-MS with an electrospray ionization mode. X-ray powder diffraction (PXRD) spectra were measured using an X-ray diffractometer (D/MAX2500, Japan) with Cu K $\alpha$  radiation operating at 40 kV and 40 mA and scanning from  $5^\circ$  to  $50^\circ$  at a rate of  $8^\circ/\text{min}$ . UV-vis absorption spectra were recorded on a Shimadzu UV-3600 spectrophotometer with a PTC-348WI temperature controller in a quartz cell (light path 10 mm) at 298 K. Photoluminescent behavior was processed on an Edinburgh Instruments FLS980 (Livingstone, UK). Quantum efficiency was measured on Edinburgh Instruments FS5. Gel permeation chromatography (GPC) was performed in aqueous on America-Waters 1525.

## 2. Recent developments in the field of near-infrared room temperature phosphorescence

**Table S1.** Detailed information of pure organic solid materials with RTP emission (phosphorescence wavelength: 600 - 900 nm) in literature.

Sample	Chemical structures	$\lambda_{\text{Phos}}$	$\tau_{\text{Phos}}$	$\Phi_{\text{PL}}$	Ref.
DTBT		616nm	39.93ms	25.0% <sup>a</sup>	[1]
BrNDI-LP		613nm	0.52 ms	3.5% <sup>a</sup>	[2]
PIth-C7 PIth-C8		622nm 634nm	0.02ms 0.49ms	33.72% 33.58%	[3]
Br-NpCzBF <sub>2</sub> I-NpCzBF <sub>2</sub>		647nm 655nm	0.58ms 0.56ms	26.0% 24.0%	[4]

t-DTBT		660nm	296ms	10.78%	[5]
BTD(OMe)-Br		648nm	585μs	3.7%	[6]
GcLP		620nm	2.49ms	—	[7]
p-TAPCB		680nm	9.87ms	47.03%	This work

[a] Phosphorescence quantum yield at rt in air.

### 3. Synthesis and Characterization

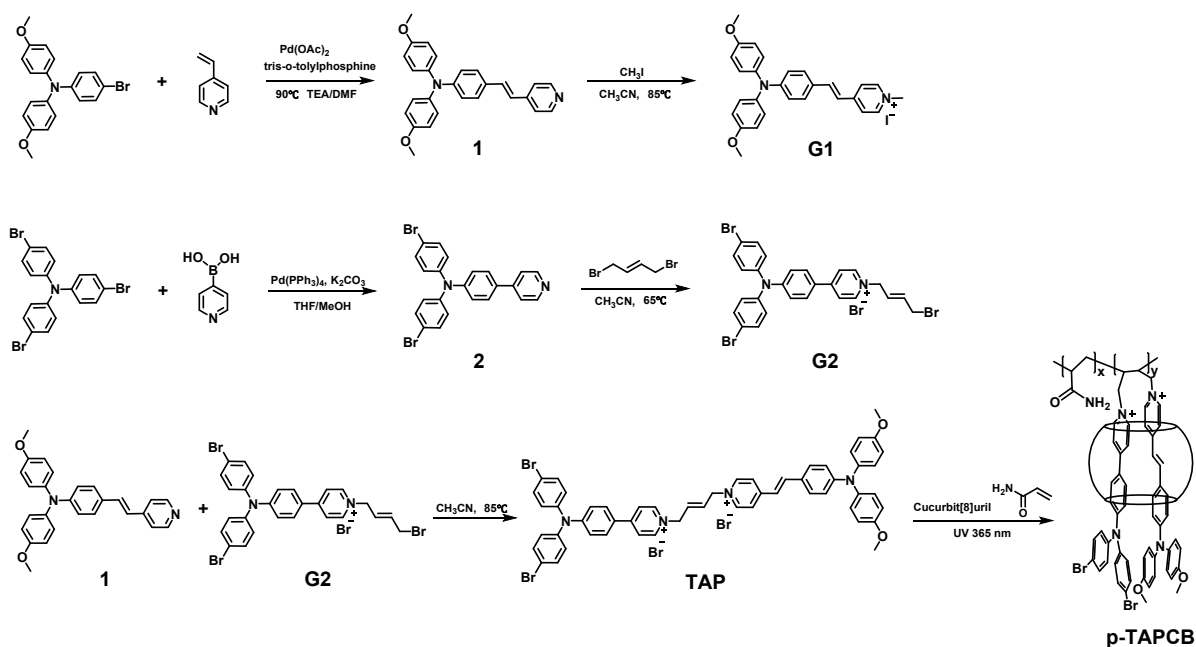


**Figure S1.** Synthetic routes of G1, G2, TAP and p-TAPCB.

*Synthesis of compound 1:* Compound 1 was synthesized according to the literature.<sup>[8]</sup> The product was obtained as a red solid (55%).

*Synthesis of compound G1:* Compound G1 was synthesized according to the literature.<sup>[9]</sup> The product was obtained as a red solid (80.5%).

*Synthesis of compound 2:* Compound 2 was synthesized according to the literature.<sup>[10]</sup> The product was obtained as a yellow solid (81%).

*Synthesis of compounds G2:* Compound 2 (100 mg, 0.21 mmol) was dissolved in CH<sub>3</sub>CN (3ml) and was slowly added dropwise to 1,4-dibromo-2-butene (225 mg, 1.05 mmol) in acetonitrile (3 ml) over 3 hours. The reaction mixture was reacted at 60 °C for 12 hours, Then, the residue was cooled to room temperature and filtered. Ethyl acetate (40ml) was added to the filtrate with a solid precipitate. The crude product was filtered and washed with ethyl acetate to obtain an orange solid (105 mg, 72%). <sup>1</sup>H NMR (400 MHz, DMSO-*d*<sub>6</sub>) δ 8.91 (d, *J* = 6.6 Hz, 2H), 8.43 (d, *J* = 6.7 Hz, 2H), 8.02 (d, *J* = 8.8 Hz, 2H), 7.61 – 7.56 (m, 4H), 7.10 (dd, *J* = 11.8, 8.7 Hz, 6H), 6.16 (t, *J* = 4.4 Hz, 2H), 5.21 (d, *J* = 4.1 Hz, 2H), 4.19 (d, *J* = 5.1 Hz, 2H).

*Synthesis of compound TAP:* Compound 1 (57 mg, 0.14 mmol) and compound G2 (69 mg, 0.10 mmol) were dissolved in 4 mL CH<sub>3</sub>CN and heated at 85 °C for 48 h. The reaction mixture was filtered while hot and washed with ethyl acetate. The crude product was recrystallized with CH<sub>3</sub>CN to obtain the red powder with a yield of 55% (61 mg). <sup>1</sup>H NMR (400 MHz, DMSO-*d*<sub>6</sub>) δ 8.92 (d, *J* = 6.5 Hz, 2H), 8.76 (d, *J* = 6.5 Hz, 2H), 8.43 (d, *J* = 6.6 Hz, 2H), 8.14 (d, *J* = 6.5 Hz, 2H), 8.02 (d, *J* = 8.6 Hz, 2H), 7.94 (d, *J* = 16.1 Hz, 1H), 7.57 (dd, *J* = 17.8, 8.4 Hz, 6H), 7.25 (s, 1H), 7.11 (q, *J* = 11.7, 10.5 Hz, 10H), 6.98 (d, *J* = 8.6 Hz, 4H), 6.74 (d, *J* = 8.5 Hz, 2H), 6.16 (s, 2H), 5.27 – 5.21 (m, 2H), 5.16 (s, 2H), 3.77 (s, 6H).; <sup>13</sup>C NMR (101 MHz, DMSO-*d*<sub>6</sub>) δ 157.22, 154.40, 154.31, 151.26, 150.78, 145.31, 144.94, 144.34, 142.09, 133.39, 130.70, 130.37, 130.33, 130.24, 128.34, 128.08, 126.19, 123.45, 123.41, 121.55, 119.45, 117.72, 117.59, 115.67, 59.80, 55.79.; HRMS (ESI) *m/z* for C<sub>54</sub>H<sub>46</sub>Br<sub>4</sub>N<sub>4</sub>O<sub>2</sub> calcd. [M-2Br]<sup>2+</sup> 471.0978, found: 471.0985.

*The general procedure of radical polymerization:* The preparation of p-TAPCB (0.5 wt%) was illustrated as a model. TAP (1.1 mg, 0.001 mmol) and CB[8] (1.34 mg, 0.001 mmol) were added to water (1 ml ) to configure the TAP/CB[8] solution (10<sup>-3</sup> M). In an argon atmosphere, p-TAPCB was prepared by copolymerization of TAP/CB[8] solution (1 ml) and acrylamide (220 mg) with 2-Hydroxy-4'-(2-hydroxyethoxy)-2-methylpropiophenone (2.2 mg) as a free radical initiator under UV

irradiation at 365 nm for 6 h. After cooling to room temperature, the mixture was added to CH<sub>3</sub>OH (10 ml) and then filtrated and washed 2~3 times with CH<sub>3</sub>OH. The crude solid was dissolved with a proper amount of distilled water (20 mL) and the resulting mixture solution was dialyzed (cut off = 5,000) against water for 3 days to remove the unreacted monomers. The solution was lyophilized and further dried under vacuum at 60°C to afford solid polymer. A similar method was employed to synthesize other supramolecular polymers like p-TAP-nCB[8], which involves preparing TAP/CB[8] solutions (10<sup>-3</sup> M) with different molar ratios (1:0.1, 1:0.2, 1:0.75) and polymerizing them with acrylamide. Similarly, in the absence of CB[8], the same method mentioned above was employed to obtain the macrocyclic-free polymers p-TAP, G1-PAM and G2-PAM.

*The general procedure of doped polymer:* PVA (10 g) was dissolved in deionized water (100 mL) at 65 °C for 5 h. The obtained PVA aqueous solutions (100 mg/mL) were used for the following experiments. Aqueous solution of TAP/CB[8] ([TAP] = 5×10<sup>-5</sup> M; [CB[8]] = 5×10<sup>-5</sup> M) was prepared for further use. Took 4 ml TAP/CB[8] (5×10<sup>-5</sup> M) and 440 µl PVA (100 mg/mL), mixed thoroughly and freeze-dried to prepare TAP/CB[8]@PVA (0.5 wt%). A similar method was performed to afford TAP/CB[8]@PAM, TAP/CB[8]@PVP. Took 4 ml G1 (5×10<sup>-5</sup> M) and G2 (5×10<sup>-5</sup> M), respectively mixed with 440 µl PAM (100 mg/mL) and then freeze-dried to prepare G1@PAM and G2@PAM (0.5 wt%).

*Preparation of transparent films of the PRET system:* p-TAPCB (10 mg/ml), TPE (3mg/ml; 0.3mg/ml; 0.03mg/ml), and PAMCz (300mg/ml; 30mg/ml; 3mg/ml) were used for the preparation of p-TAPCB doped systems with different doping ratios. The films were produced with the drop-casting approach on quartz flakes (1cm×1cm, 0.5 ml solution). After drying at 85 °C for 6 h, the transparent films were obtained.

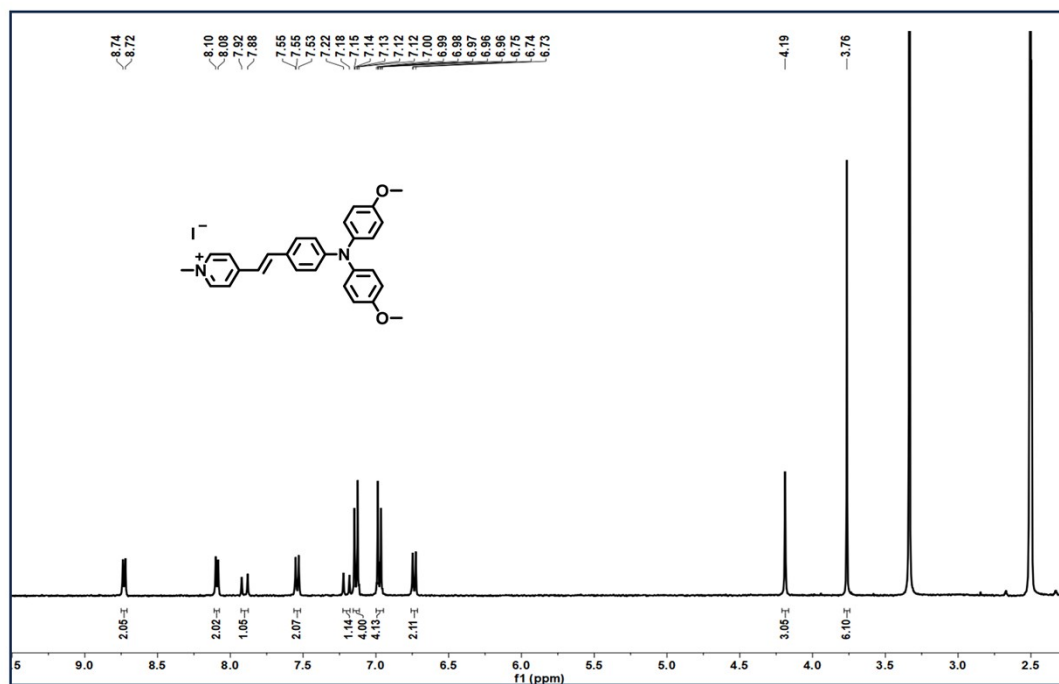


**Figure S2.**  $^1\text{H}$  NMR spectra (400 MHz,  $\text{DMSO-}d_6$ , 298 K) of compound G1.

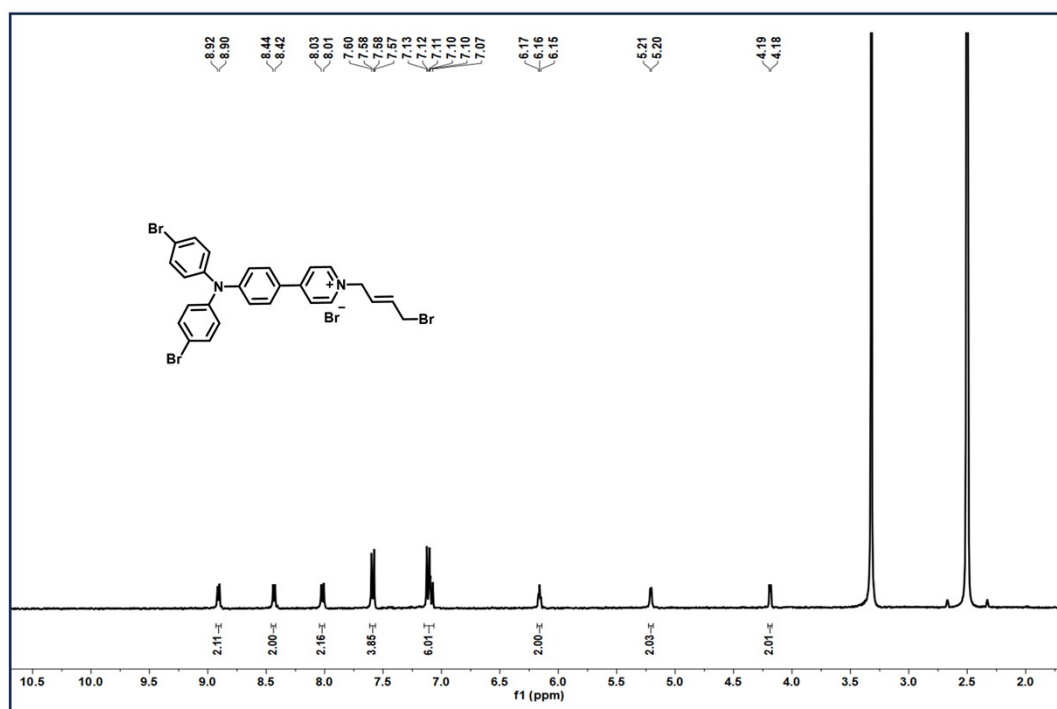


**Figure S3.** (a)  $^1\text{H}$  NMR spectrum (400 MHz,  $\text{DMSO-}d_6$ , 298 K) of compound G2.

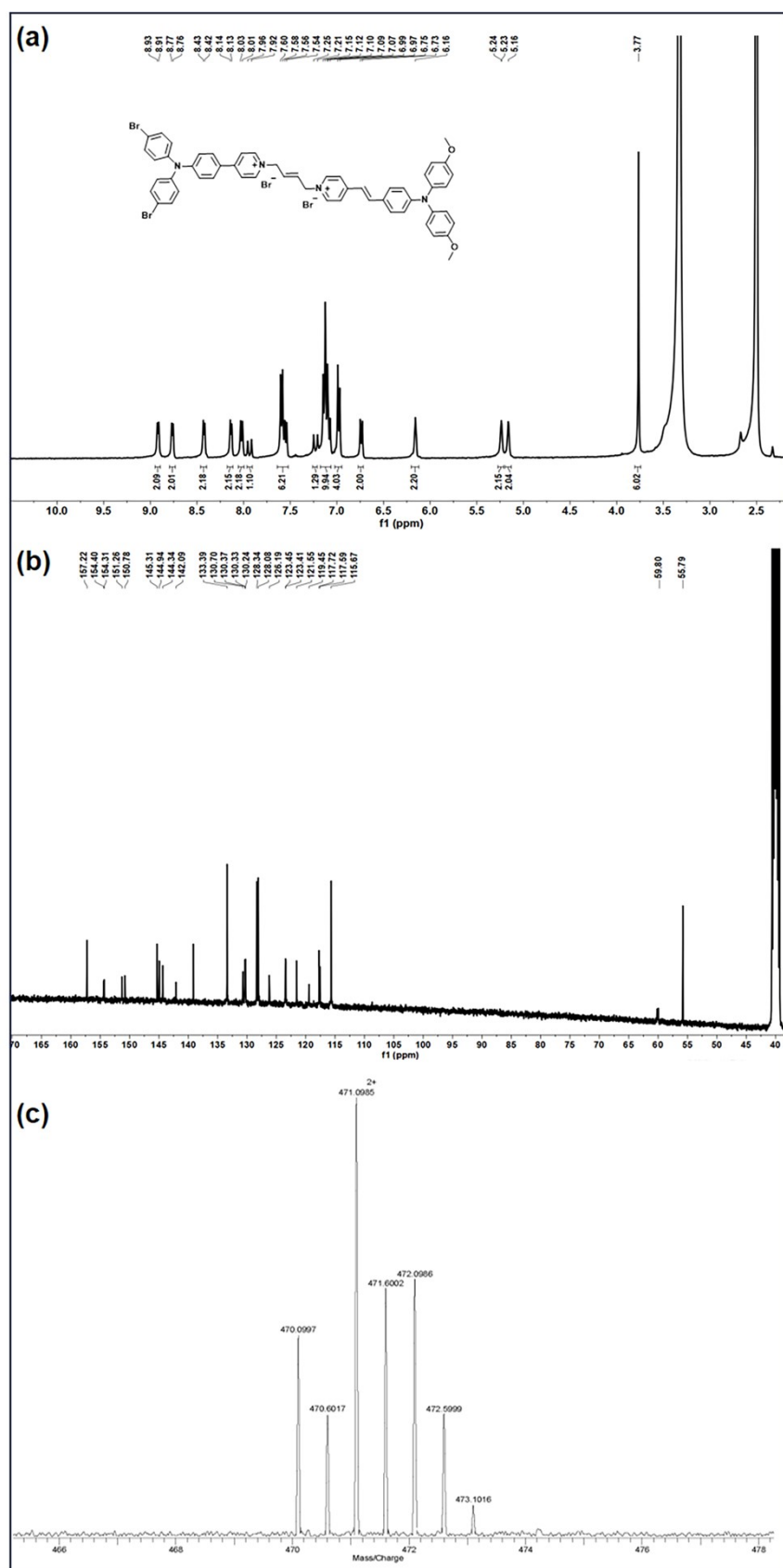


**Figure S4.** (a)  $^1\text{H}$  NMR spectrum (400 MHz, DMSO- $d_6$ , 298 K), (b)  $^{13}\text{C}$  NMR spectrum (400 MHz, DMSO- $d_6$ , 298 K), (c) HRMS (ESI) spectrum of TAP.

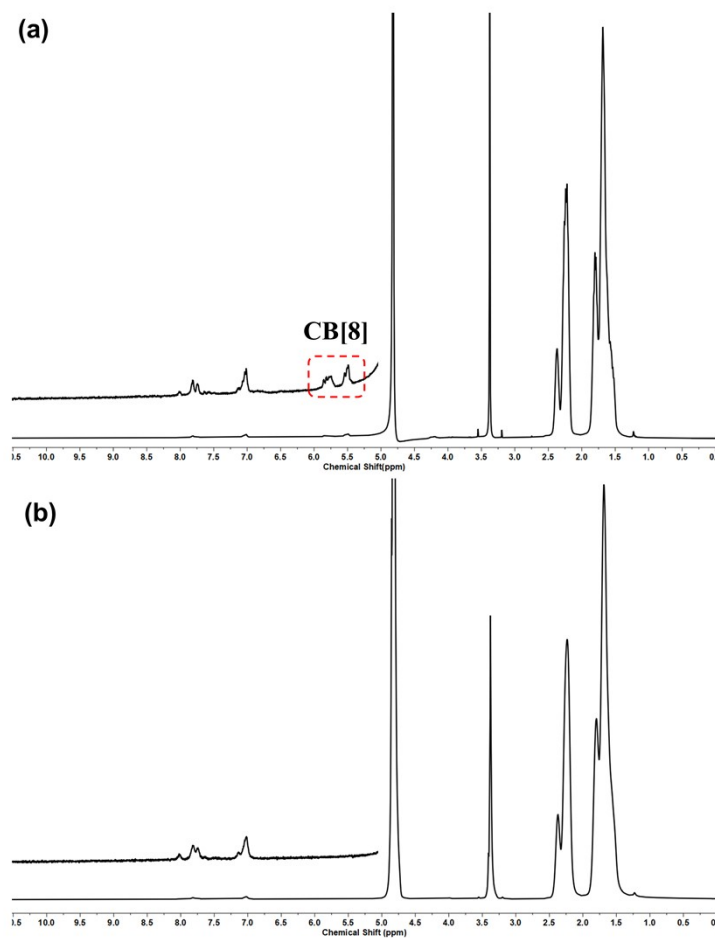


**Figure S5.**  $^1\text{H}$  NMR spectra (400 MHz,  $\text{D}_2\text{O}$ , 298 K) of p-TAPCB ( $y/x = 0.16\%$ ) (a) and p-TAP (b).

**Table S2.** Characterizations of polymers p-TAPCB by aqueous GPC.

Sample	Mp	Mn	Mw	Mz	Mz+1	Mv	PD
p-TAPCB	731840	116421	463847	807249	1032492	410902	410902

#### 4. Assembly behavior and Luminescent properties of copolymers

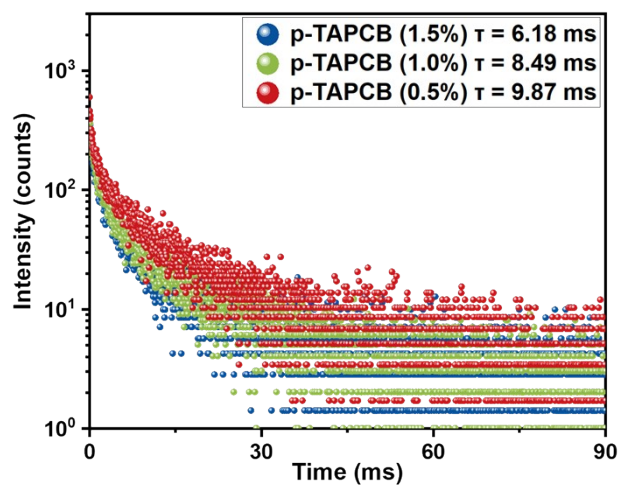




**Figure S6.** The time-correlated decay curves of p-TAPCB at 680 nm with different monomer mass ratios. ( $\lambda_{\text{ex}} = 480$  nm, recorded at 680 nm).

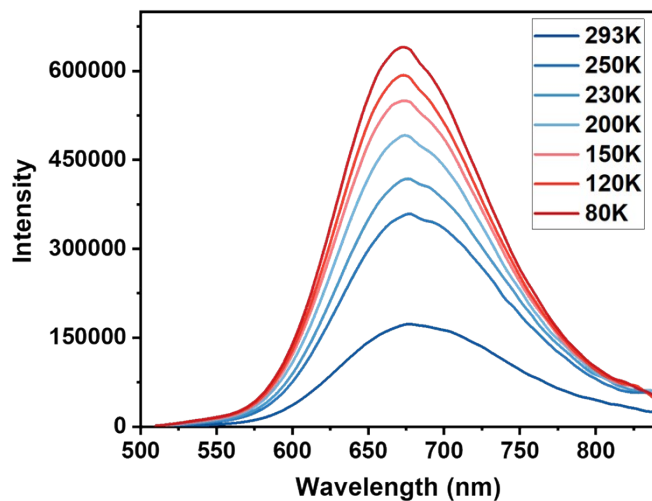


**Figure S7.** Temperature-dependent emission spectra of copolymer p-TAPCB. ( $\lambda_{\text{ex}} = 480$  nm).

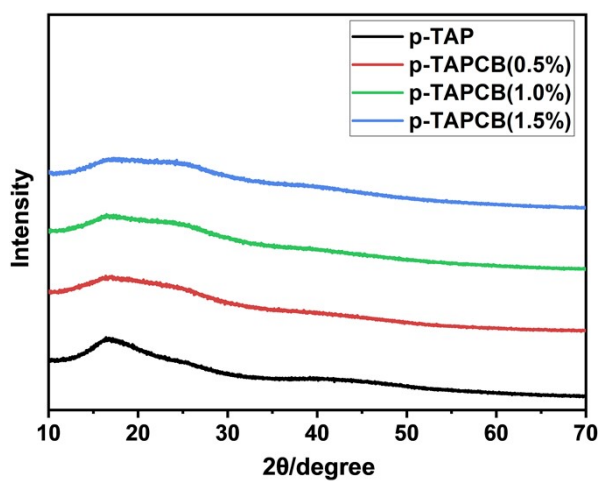


**Figure S8.** XRD patterns of p-TAPCB and p-TAP.

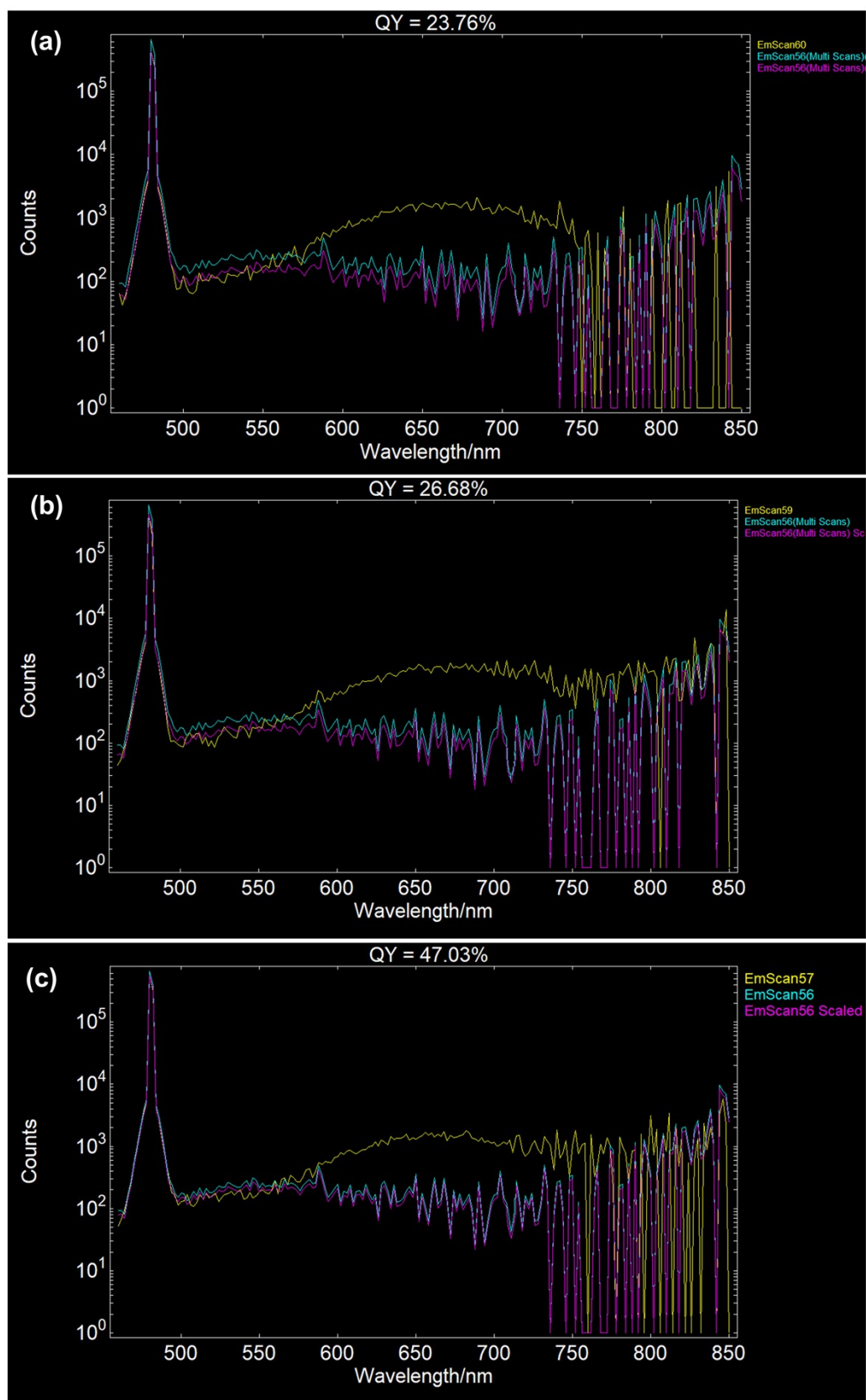


**Figure S9.** The photoluminescence quantum yield of p-TAPCB with different monomer ratios: (a) p-TAPCB-1.5%; (b) p-TAPCB-1.0%; (c) p-TAPCB-0.5%.

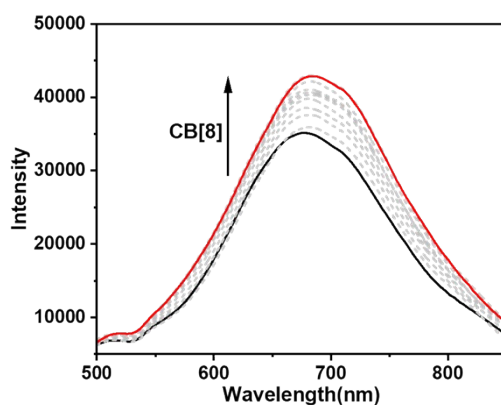


**Figure S10.** PL spectra of TAP/CB[8] upon the addition of 0 to 11  $\mu\text{M}$  CB[8]. ( $\lambda_{\text{ex}} = 450 \text{ nm}$ , [TAP] = 10  $\mu\text{M}$ ).

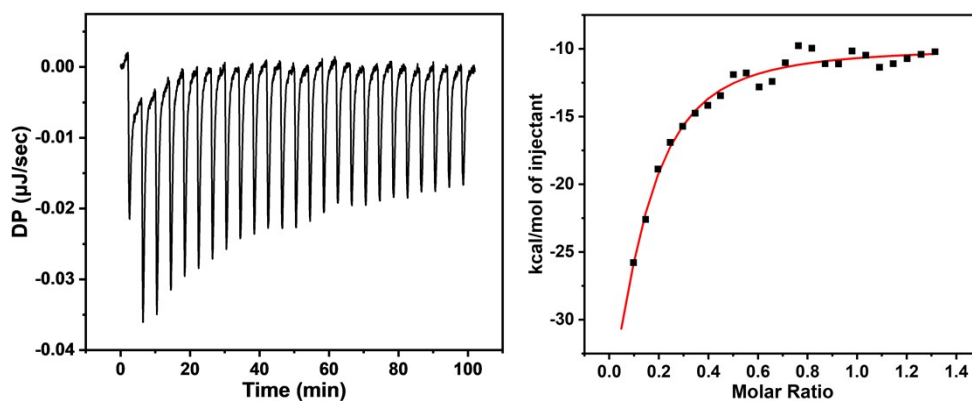


**Figure S11.** ITC isotherms for the titration of TAP with CB[8] at 298 K in  $\text{H}_2\text{O}$ .

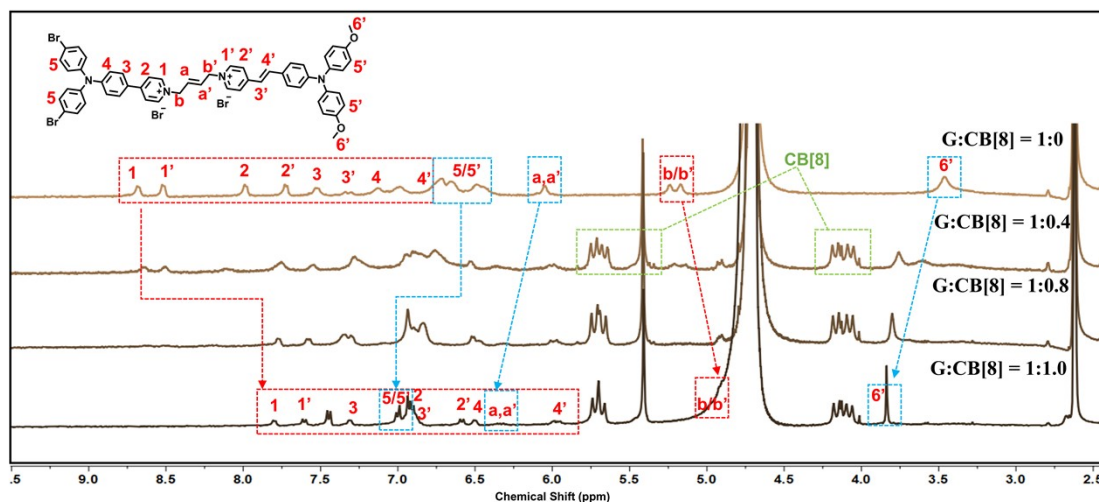


**Figure S12.**  $^1\text{H}$  NMR spectral changes of TAP after adding 0, 0.4, 0.8, 1.0 equiv CB[8]. ([TAP] = 0.5 mM, 400 MHz,  $\text{D}_2\text{O}$ -5%DMSO- $d_6$ , 298 K).

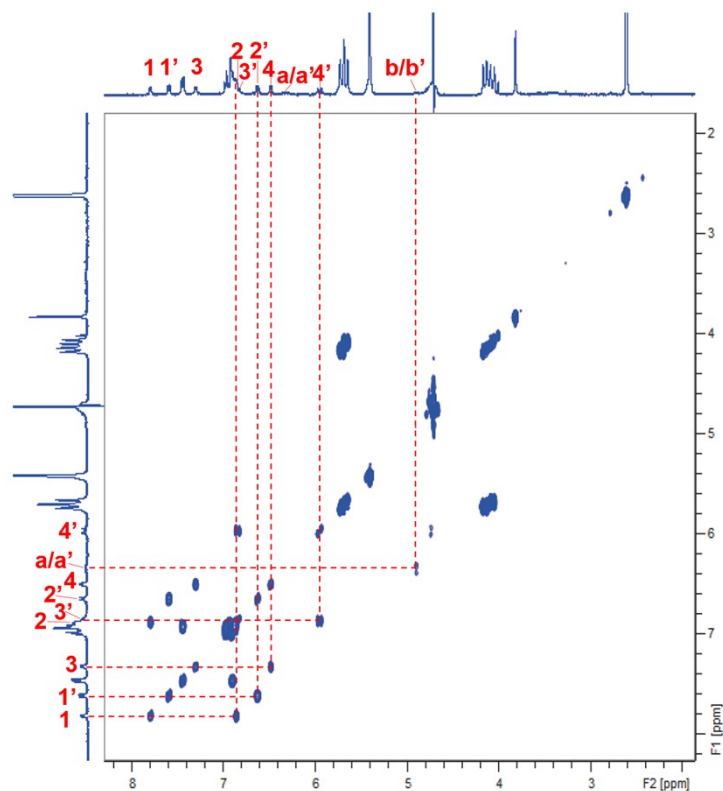


**Figure S13.** COSY spectrum (400 MHz, D<sub>2</sub>O-5%DMSO-*d*<sub>6</sub>, 298 K) of TAP/CB[8] ([TAP] = [CB[8]] = 0.5 mM).

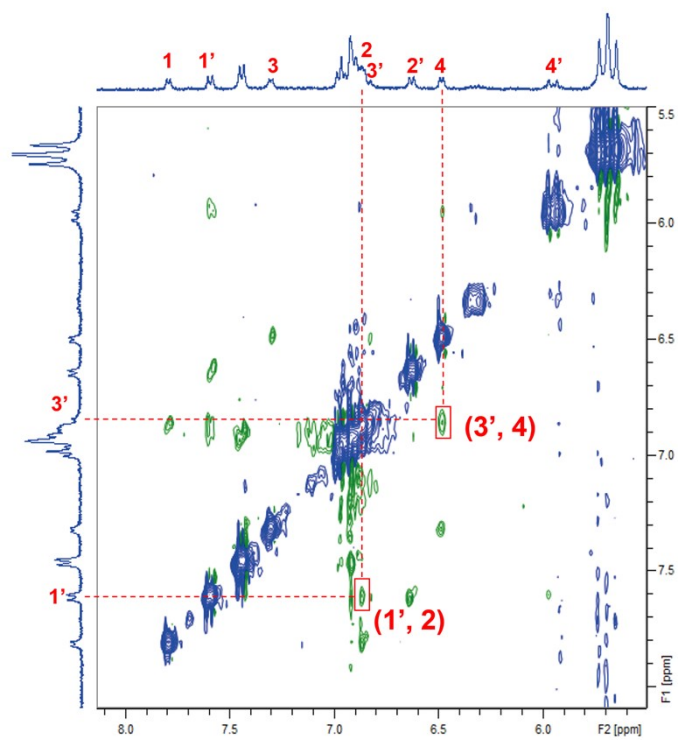


**Figure S14.** ROESY spectrum (400 MHz, D<sub>2</sub>O-5%DMSO-*d*<sub>6</sub>, 298 K) of TAP/CB[8] ([TAP] = [CB[8]] = 0.5 mM).

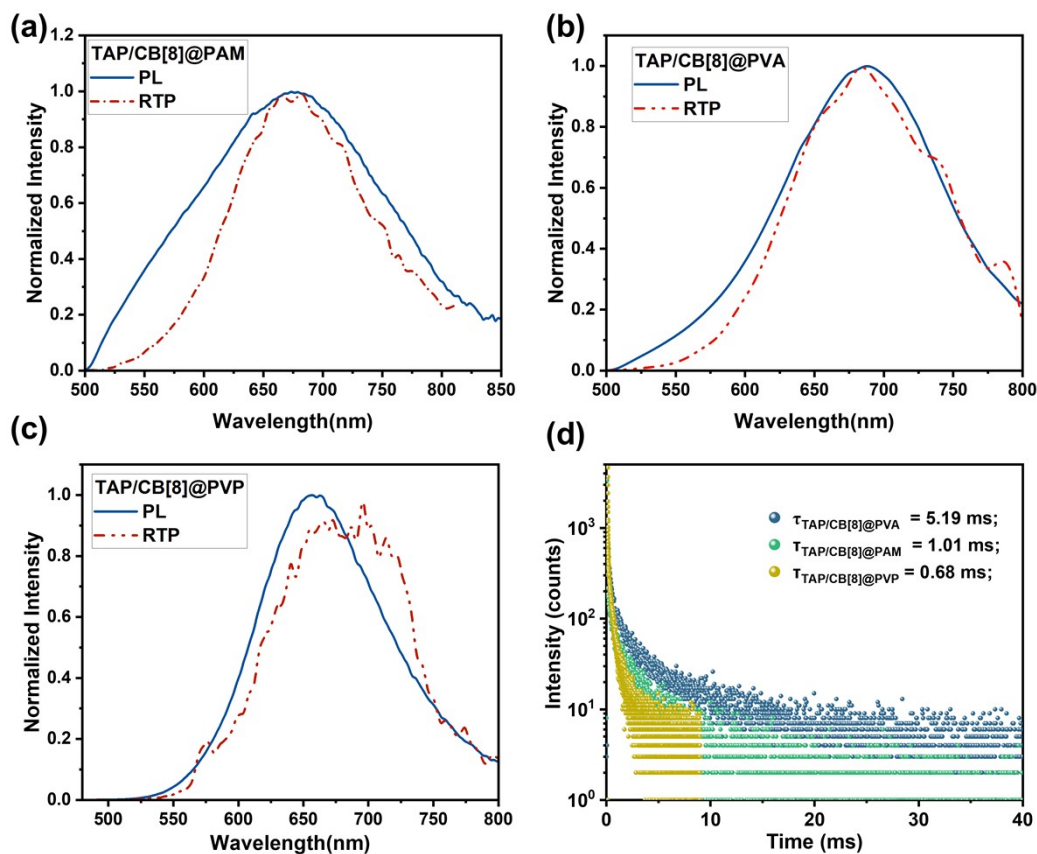


**Figure S15.** (a-c) The steady-state PL and the delayed spectra of TAP/CB[8]@PAM, TAP/CB[8]@PVA, and TAP/CB[8]@PVP. (d) The time-correlated decay curves of TAP/CB[8]@PVA, TAP/CB[8]@PAM and TAP/CB[8]@PVP ( $\lambda_{\text{em}} = 680 \text{ nm}$ ).

**Table S3.** Luminescent properties and composition of doping systems and copolymers based on TAP/CB[8]

Doping System	Composition	Excitation	Phosphorescence	$\tau_{\text{Phos}}$	$\phi_{\text{PL}}$
TAP/CB[8]@PVA	TAP:CB[8]=1:1	480nm	680nm	5.19ms	14.59%
TAP/CB[8]@PAM	TAP:CB[8]=1:1	480nm	680nm	1.03ms	3.87%
TAP/CB[8]@PVP	TAP:CB[8]=1:1	480nm	680nm	0.68ms	3.31%
Copolymer	Composition	Excitation	Phosphorescence	$\tau_{\text{Phos}}$	$\phi_{\text{PL}}$
p-TAPCB	TAP:CB[8]=1:1	480nm	680nm	9.87ms	47.03%
p-TAP	TAP:CB[8]=1:0	280nm; 430nm	440nm; 560nm	341.68ms; 5.93ms	10.53%
p-TAP-0.2CB[8]	TAP:CB[8]=1:0.2	280nm; 430nm; 480nm	440nm; 560nm; 640nm	211.01ms; 12.05ms; 11.73ms	—
p-TAP-0.75CB[8]	TAP:CB[8]=1:0.75	280nm; 430nm; 480nm	440nm; 560nm; 650nm	189.39ms; 17.83ms; 13.47ms	—

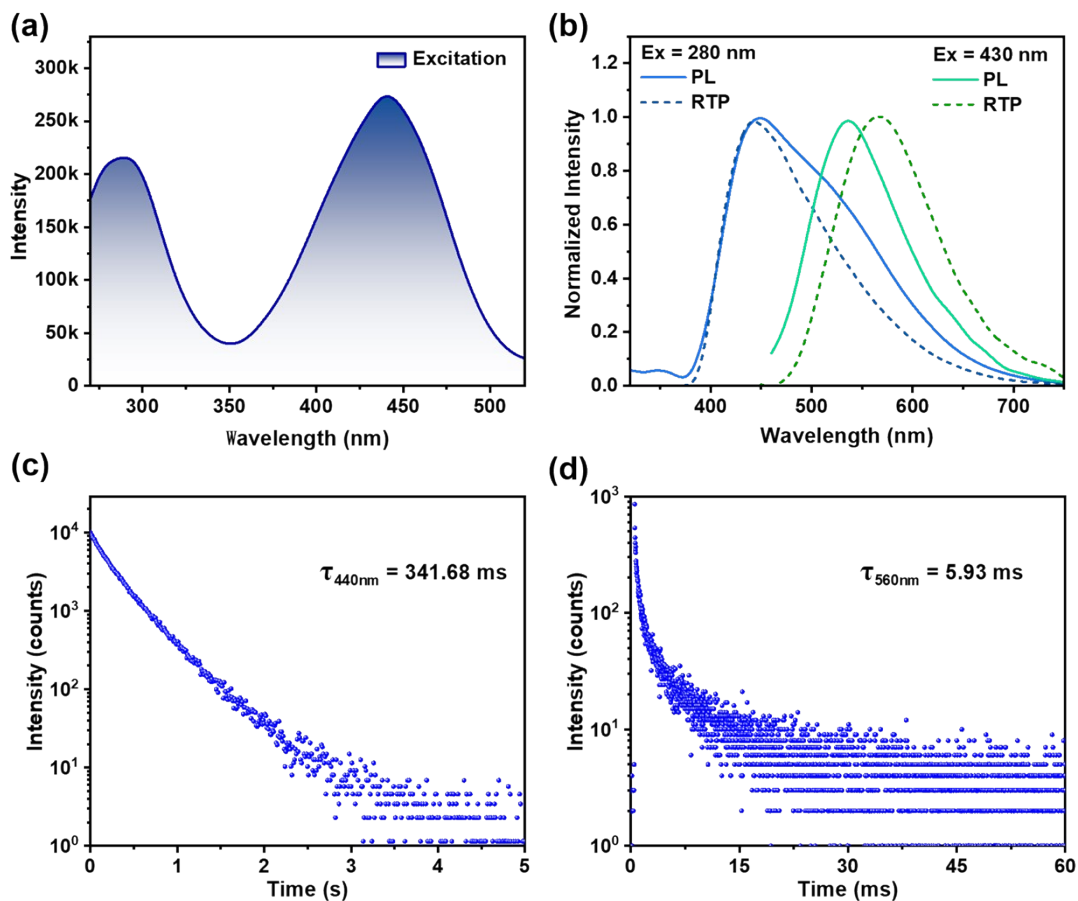


**Figure S16.** (a) The excitation spectrum of p-TAP. (b) The steady-state PL and phosphorescence spectra of p-TAP ( $\lambda_{\text{ex}} = 280 \text{ nm}$  or  $430 \text{ nm}$ ; delay time = 1 ms); (c, d) The time-correlated decay curves of p-TAP (recorded at 440 nm ( $\lambda_{\text{ex}} = 280 \text{ nm}$ ), recorded at 560 nm ( $\lambda_{\text{ex}} = 430 \text{ nm}$ )).

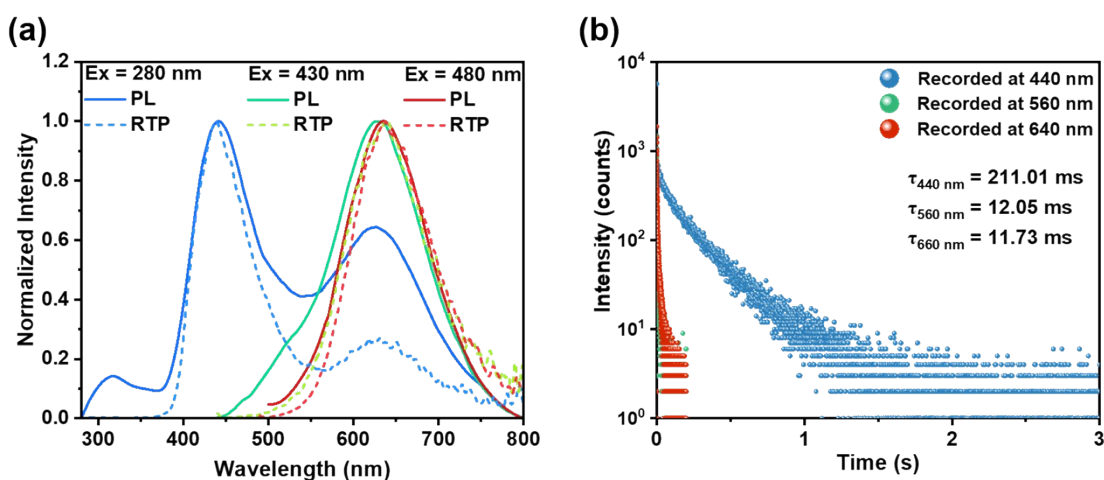


**Figure S17.** (a) The steady-state PL and delayed spectra of p-TAP-0.2CB[8] ( $\lambda_{\text{ex}} = 280 \text{ nm}$ ,  $430 \text{ nm}$ ,  $480 \text{ nm}$ ; delay time = 1 ms); (b) The time-correlated decay curves of p-TAP-0.2CB[8] (recorded at 440 nm ( $\lambda_{\text{ex}} = 280 \text{ nm}$ ), recorded at 560 nm ( $\lambda_{\text{ex}} = 430 \text{ nm}$ ) and 640 nm ( $\lambda_{\text{ex}} = 480 \text{ nm}$ )).



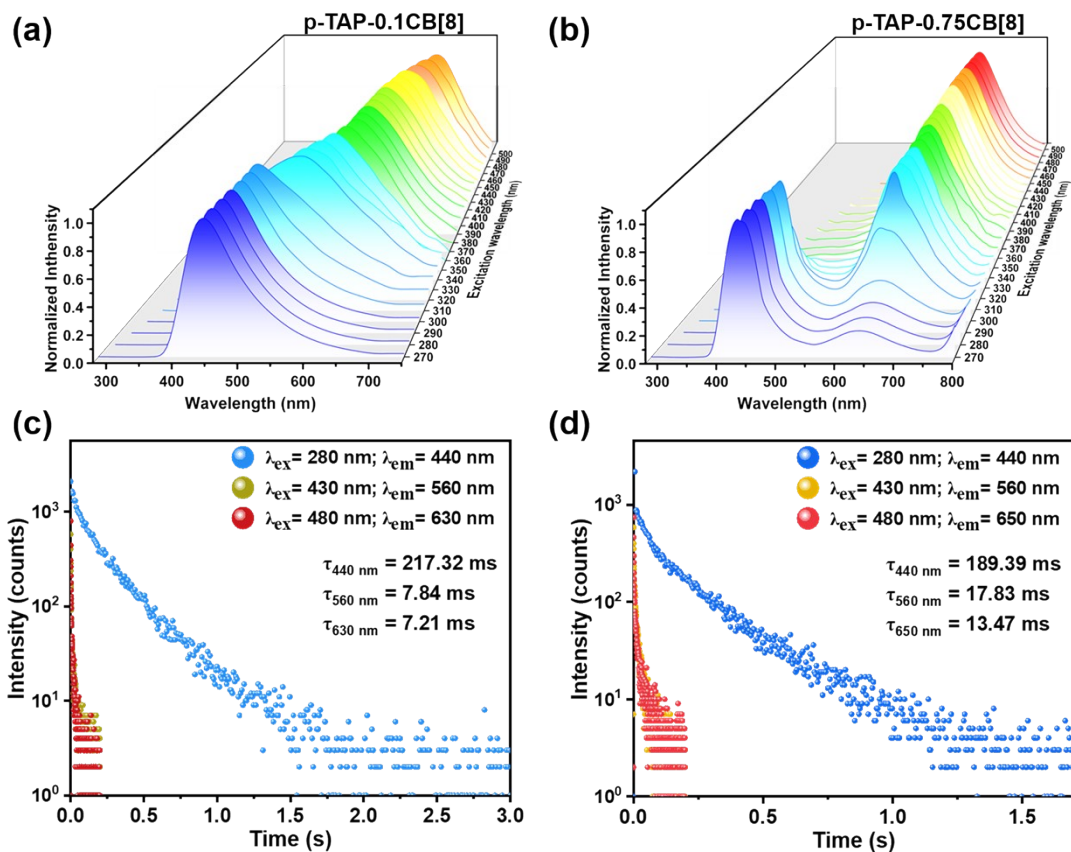


**Figure S18.** (a, b) Phosphorescence spectra of the polymers p-TAP-0.1CB[8] (a) and p-TAP-0.75CB[8] (b) at different excitation wavelengths. (c, d) The time-correlated decay curves of p-TAP-0.1CB[8] (c) and p-TAP-0.75CB[8] (d).

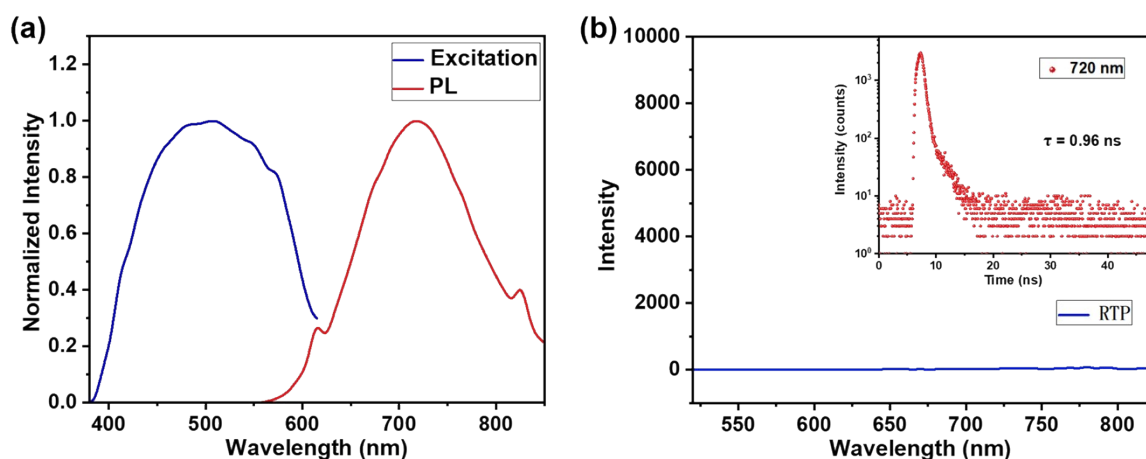


**Figure S19.** (a) The excitation spectrum and steady-state PL spectrum of the doping system G1@PAM. (b) The delayed spectrum and time-correlated decay curves of doping system G1@PAM (recorded at 720 nm).

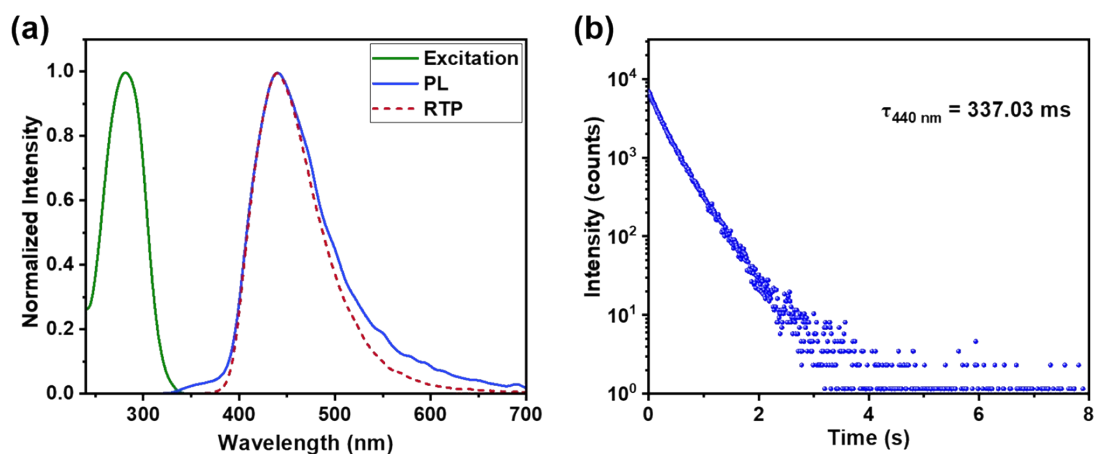


**Figure S20.** (a) The excitation spectrum, steady-state PL spectrum and the delayed spectrum of polymerization system G1-PAM ( $\lambda_{\text{ex}} = 280 \text{ nm}$ ; delay time = 1 ms). (b) The time-correlated decay curves of polymerization system G1-PAM (recorded at 440 nm).

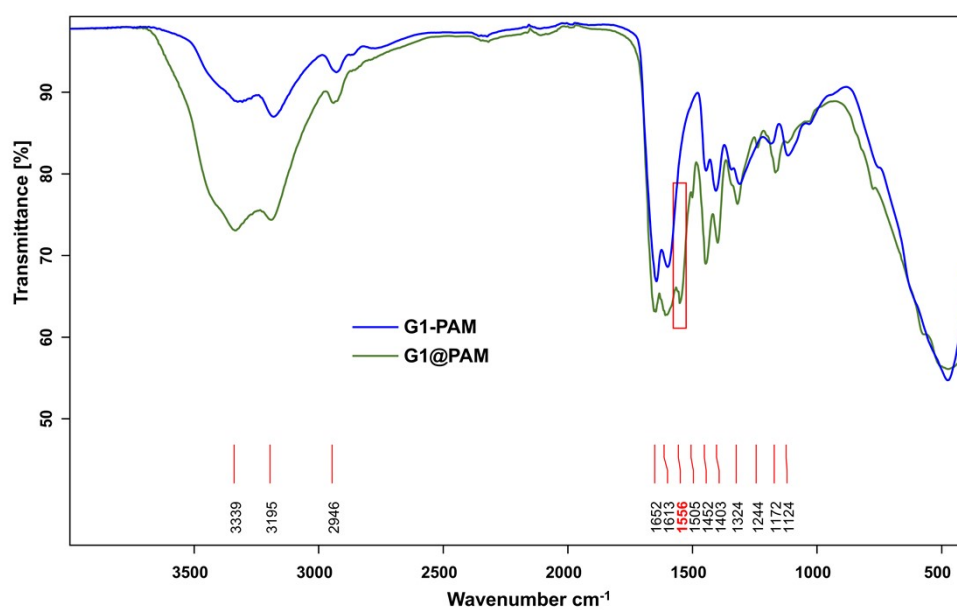


**Figure S21.** Fourier transform infrared (FTIR) spectra of doping system G1@PAM and polymerization system G1-PAM.



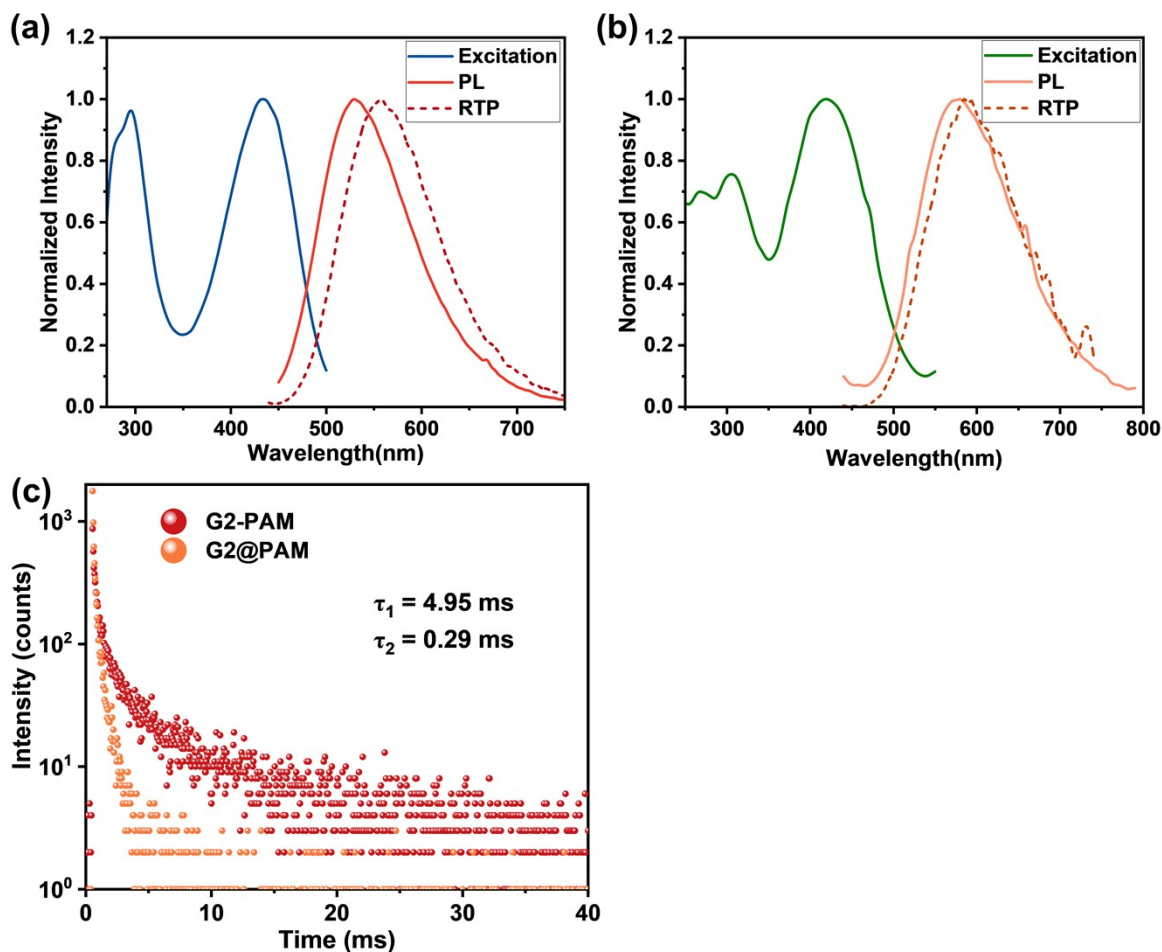


**Figure S22.** (a) The excitation spectrum, steady-state PL spectrum and the phosphorescence spectrum of polymerization system G2-PAM; (b) The excitation spectrum, steady-state PL spectrum and the delayed spectrum of doping system G2@PAM. (delay time = 1 ms); (c) The time-correlated decay curves of G2-PAM and G2@PAM.

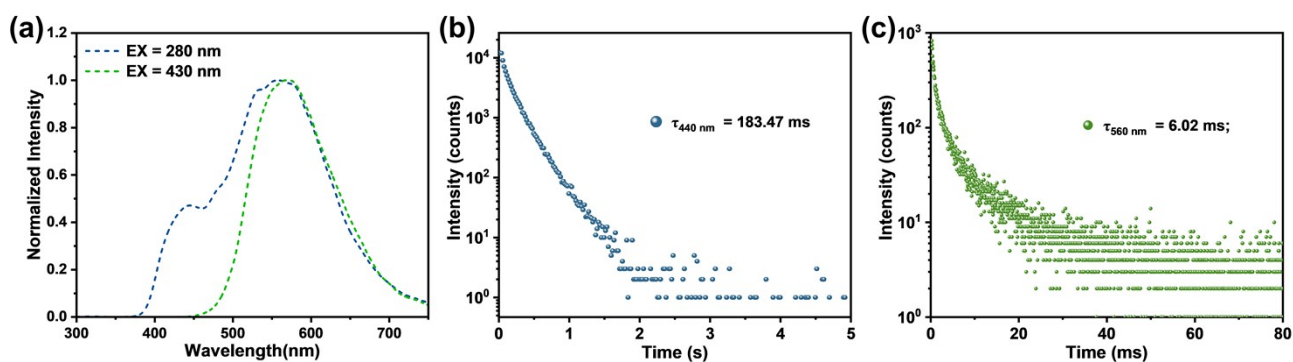


**Figure S23.** (a) The steady-state PL and phosphorescence spectra of p-TAP-CB[7] ( $\lambda_{\text{ex}}$  = 280 nm or 430 nm; delay time = 1 ms); (b, c) The time-correlated decay curves of p-TAP-CB[7] (recorded at 440 nm ( $\lambda_{\text{ex}}$  = 280 nm), recorded at 560 nm ( $\lambda_{\text{ex}}$  = 430 nm)).

## 5. Phosphorescence resonance energy transfer

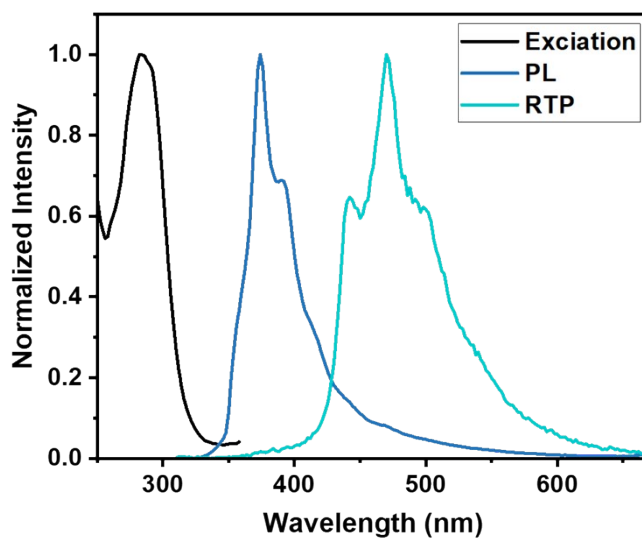


**Figure S24.** The excitation spectrum, PL spectrum, and phosphorescence spectrum of TPE doped in PAM.

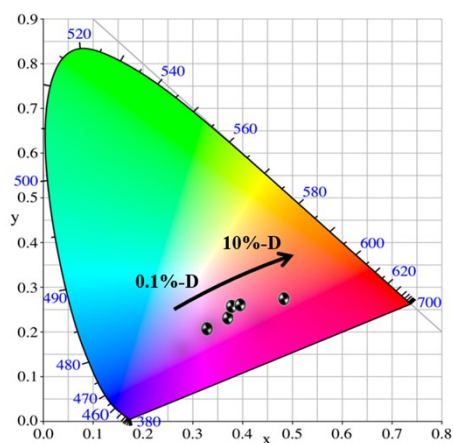


**Figure S25.** CIE 1931 chromaticity diagram of p-TAPCB-TPE with different doping mass ratios of TPE based on phosphorescence spectra in Figure 5b (D: TPE).

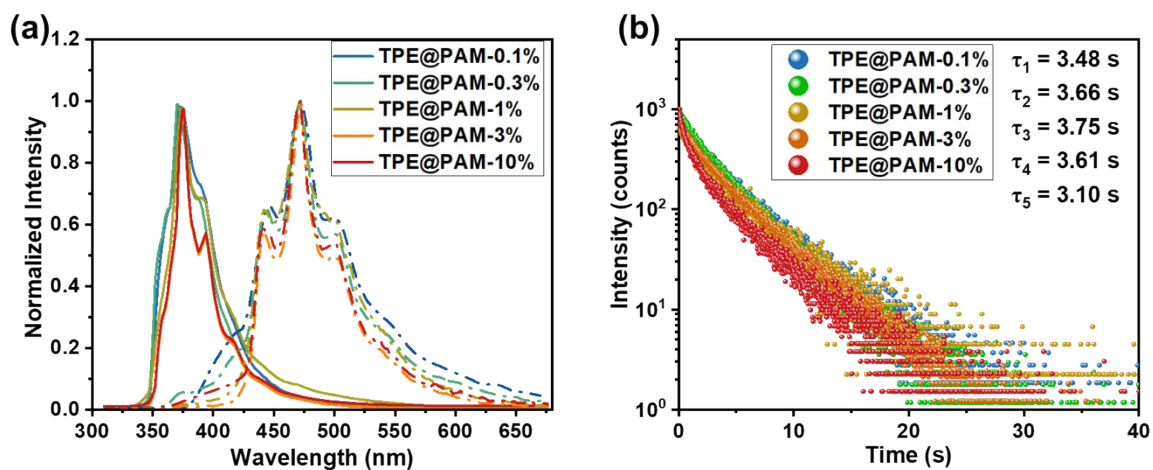


**Figure S26.** (a) The PL spectra and phosphorescence spectra of TPE@PAM with different mass ratios. (b) The time-correlated decay curves of TPE@PAM with different mass ratios ( $\lambda_{\text{ex}} = 290$  nm; recorded at 470 nm).

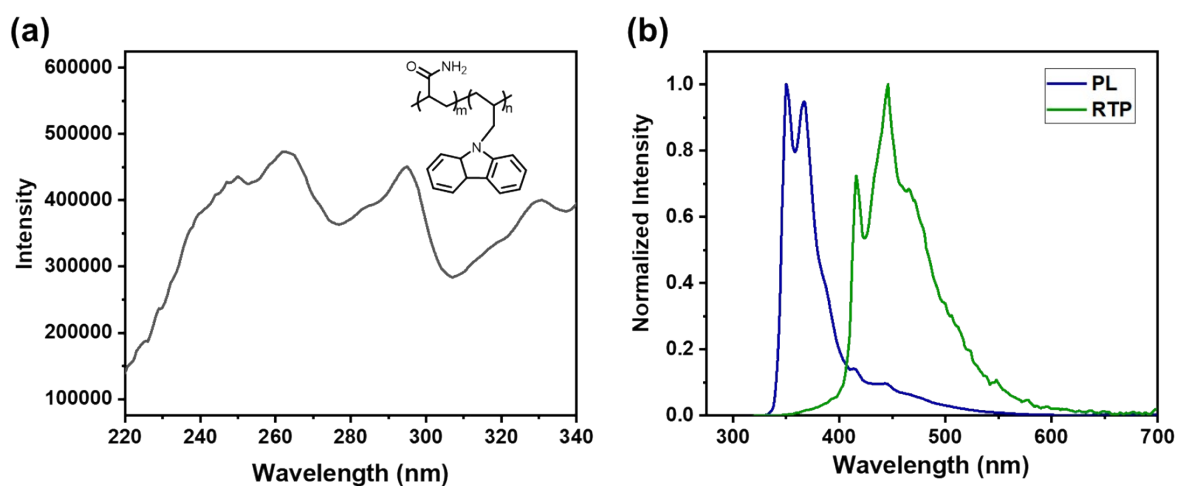


**Figure S27.** (a) The excitation spectrum of PAMCz. (b) The PL spectra and phosphorescence spectra of PAMCz.

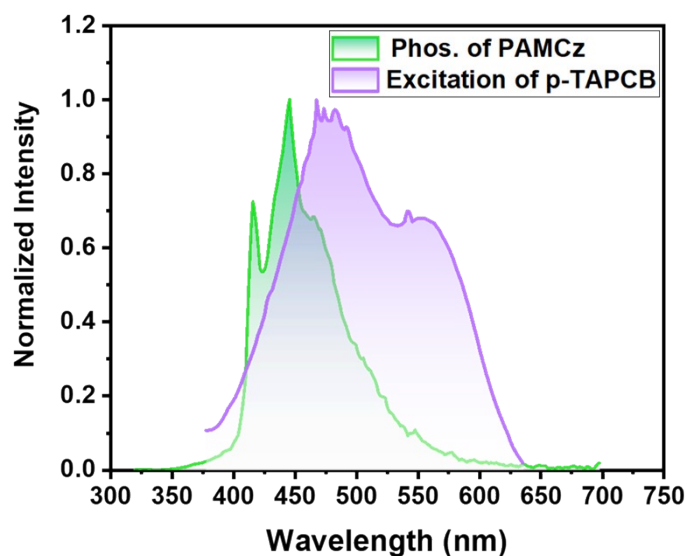


**Figure S28.** The phosphorescence spectra of PAMCz ( $\lambda_{\text{ex}} = 290$  nm) and the excitation spectrum of p-TAPCB.

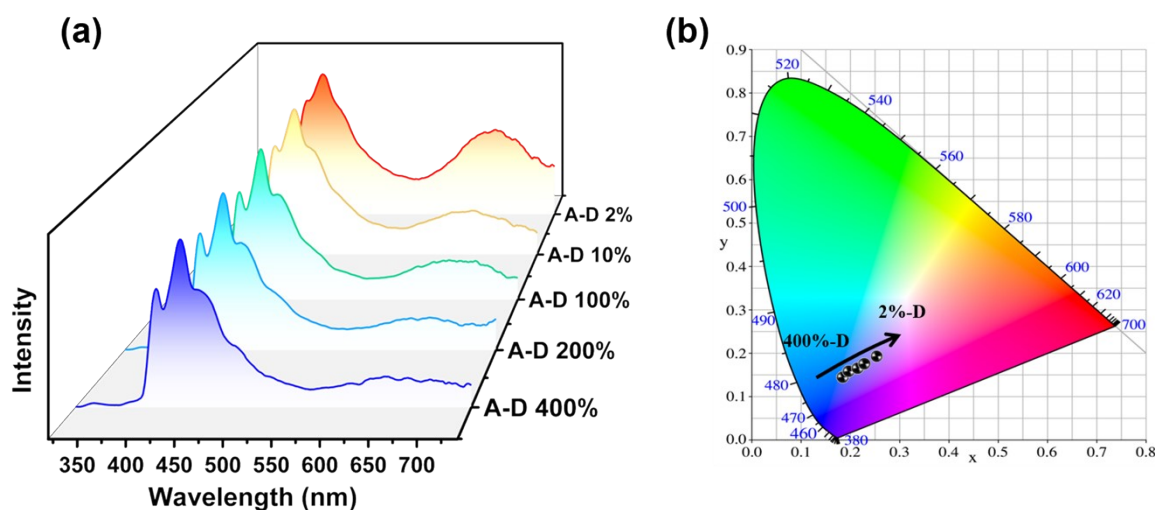


**Figure S29.** (a) Delayed spectra of PAMCz-doped systems (p-TAPCB-PAMCz) with different doping weight concentrations of PAMCz ( $\lambda_{\text{ex}} = 290$  nm, delay time = 1 ms, normalized at 450 nm, A: p-TAPCB; D: PAMCz); (b) CIE 1931 chromaticity diagram of p-TAPCB-PAMCz based on phosphorescence spectra in figure (a).

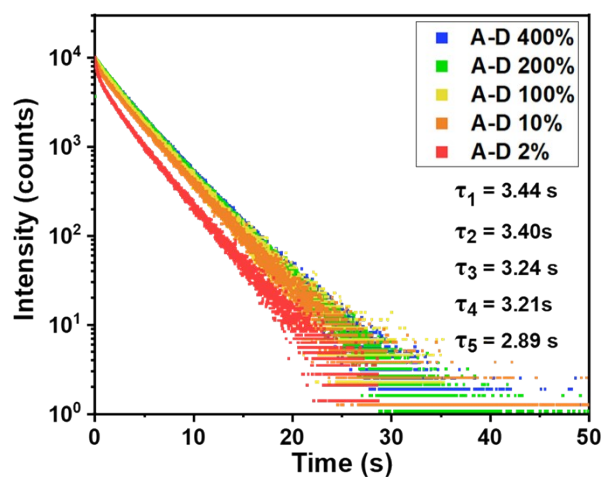


**Figure S30.** The time-correlated decay curves of p-TAPCB-PAMCz at 450 nm with different mass ratios of PAMCz (A: p-TAPCB; D: PAMCz;  $\lambda_{\text{ex}} = 290$  nm).

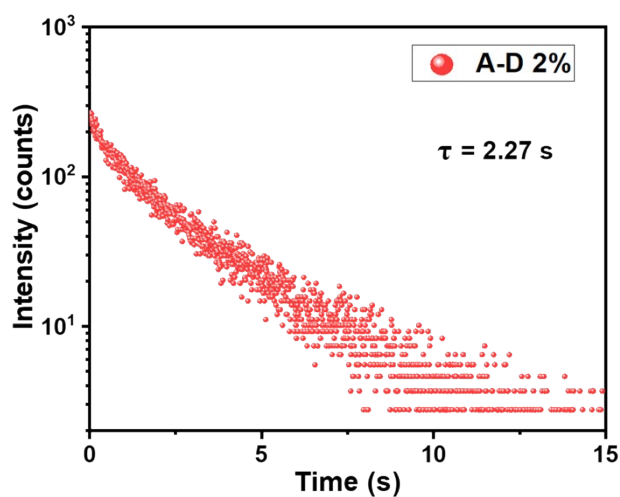


**Figure S31.** The time-correlated decay curves of p-TAPCB-PAMCz (2wt%) films ( $\lambda_{\text{ex}} = 290$  nm, A: p-TAPCB; D: PAMCz).



**Figure S32.** Photographs of p-TAPCB-PAMCz (2%) under 300 nm UV light and the afterglow after turning off the UV light.

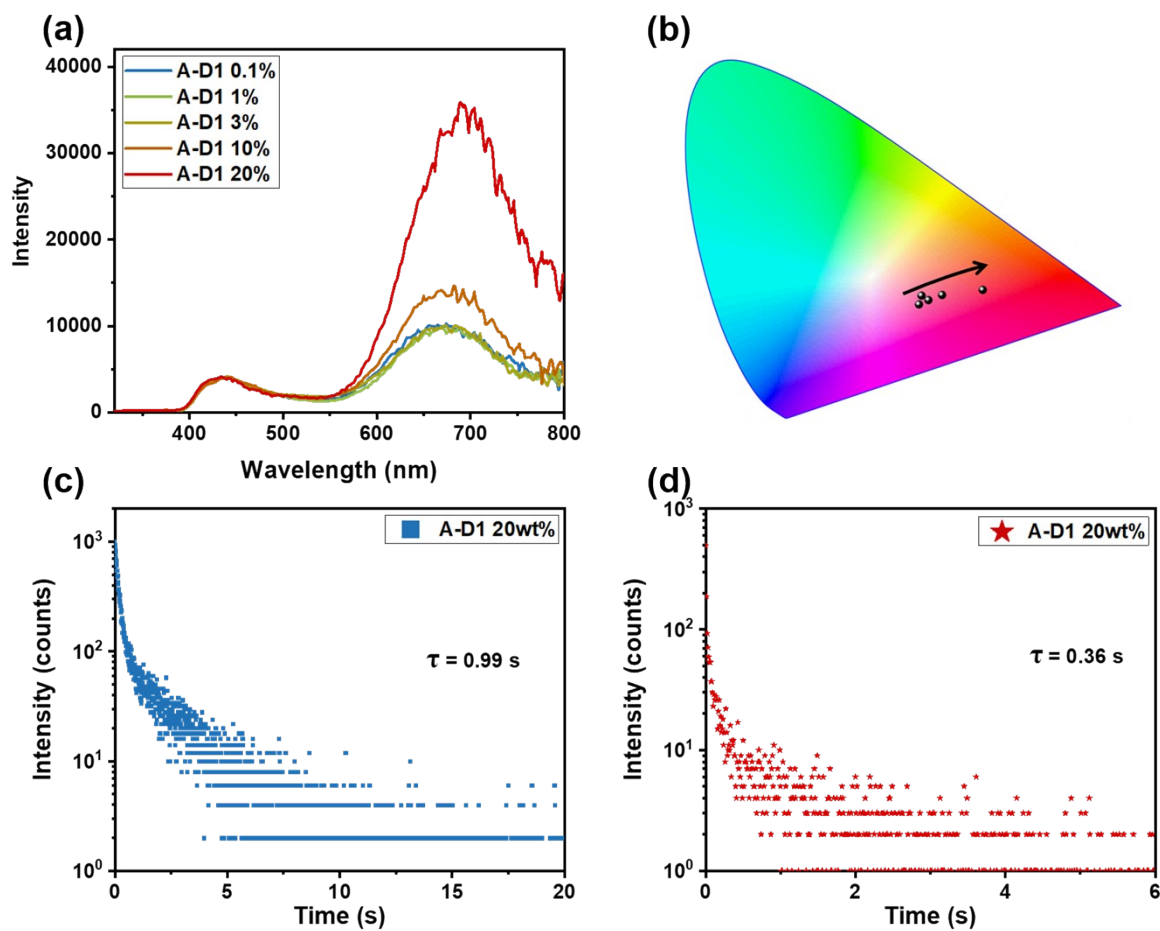


**Figure S33.** (a) The delayed spectrum of p-TAPCB(1.5%)-TPE with doping weight concentrations (wt%) ( $\lambda_{\text{ex}} = 290$  nm, normalized at 450 nm); (b) CIE 1931 chromaticity diagram of the delayed spectrum in figure a; (c, d) The time-correlated decay curves of p-TAPCB(1.5%)-TPE (20 wt%) at 450 nm (c) and 680nm (A: p-TAPCB; D1: TPE;  $\lambda_{\text{ex}} = 290$  nm).

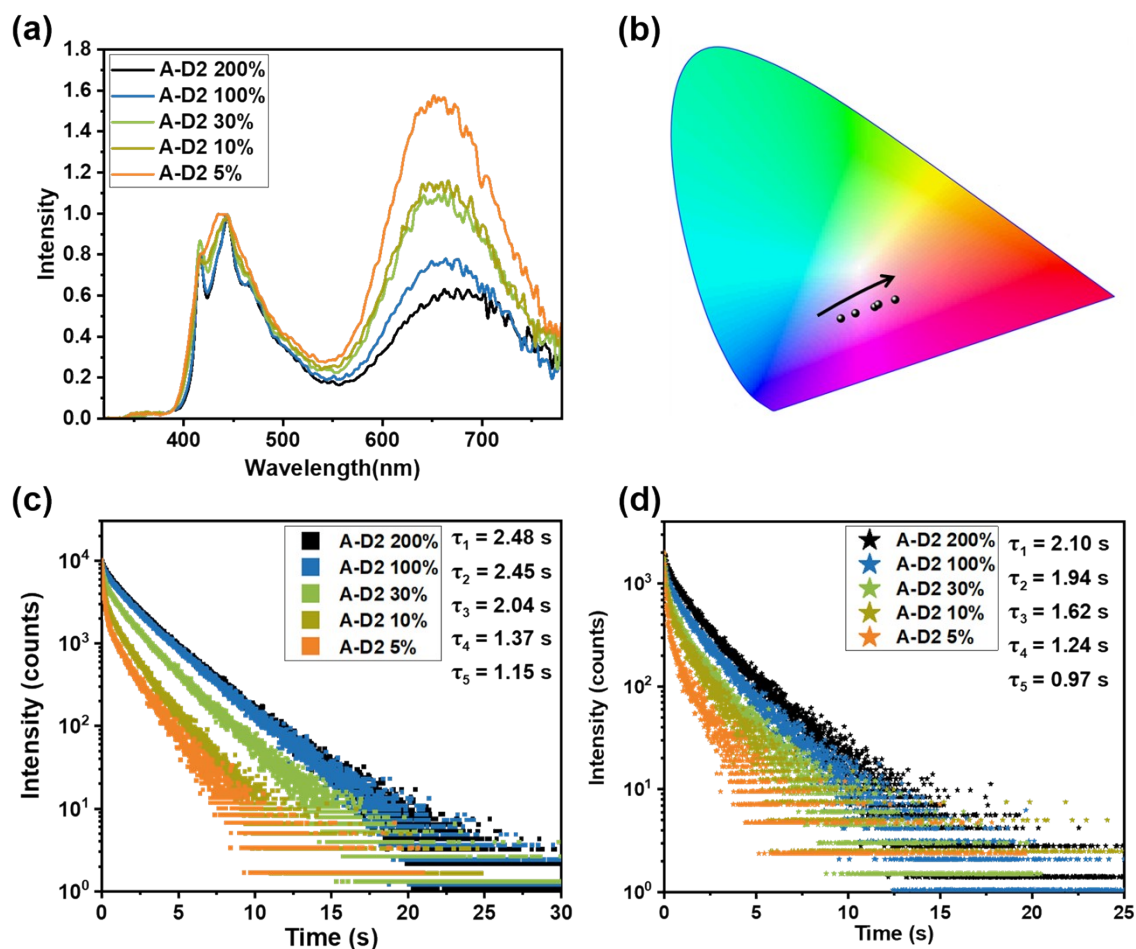


**Figure S34.** (a) The delayed spectrum of p-TAPCB(1.5%)-PAMCz with different doping weight concentrations (wt%) ( $\lambda_{\text{ex}} = 290$  nm, normalized at 450 nm); (b) CIE 1931 chromaticity diagram of the delayed spectrum in figure a; The time-correlated decay curves of p-TAPCB(1.5%) at 450 nm (c) and 680nm (d) with different mass ratios of PAMCz (A: p-TAPCB; D2: PAMCz;  $\lambda_{\text{ex}} = 290$  nm).

**Table S4.** Photophysical properties of energy transfer systems.

Sample	$\lambda_{\text{ex}}$	$\lambda_{\text{phos}}$	$\tau_{680\text{nm}}$
p-TAPCB	480nm	680nm	9.87ms
p-TAPCB-0.5%/PAMCz (2%)	290nm	450nm, 680nm	2.27s
p-TAPCB-1.5%/ PAMCz (5%)	290nm	450nm, 680nm	0.97s
p-TAPCB-0.5%/TPE (10%)	290nm	450nm, 680nm	1.49s
p-TAPCB-1.5%/TPE (20%)	290nm	450nm, 680nm	0.36s

## 6. Reference

1. G. He, L. Du, Y. Gong, Y. Liu, C. Yu, C. Wei, W. Z. Yuan, Crystallization-induced red phosphorescence and grinding-induced blue-shifted emission of a benzobis(1,2,5-thiadiazole)-thiophene conjugate. *ACS Omega* **2019**, 4, 344-351.
2. S. Kuila, K. V. Rao, S. Garain, P. K. Samanta, S. Das, S. K. Pati, M. Eswaramoorthy, S. J. George, Aqueous phase phosphorescence: ambient triplet harvesting of purely organic phosphors via supramolecular scaffolding. *Angew. Chem., Int. Ed.* **2018**, 57, 17115-17119.
3. Y. Yu, Y. Fan, C. Wang, Y. Wei, Q. Liao, Q. Li, Z. Li, Achieving enhanced ML or RTP performance: alkyl substituent effect on the fine-tuning of molecular packing. *Mater. Chem. Front.* **2021**, 5, 817-824.
4. X.-F. Wang, H. Xiao, P.-Z. Chen, Q.-Z. Yang, B. Chen, C.-H. Tung, Y.-Z. Chen, L.-Z. Wu, Pure organic room temperature phosphorescence from excited dimers in self-assembled nanoparticles under visible and near-infrared irradiation in water. *J. Am. Chem. Soc.* **2019**, 141, 5045-5050.
5. Y. Fan, S. Liu, M. Wu, L. Xiao, Y. Fan, M. Han, K. Chang, Y. Zhang, X. Zhen, Q. Li, Z. Li, Mobile phone flashlight-excited red afterglow bioimaging. *Adv. Mater.* **2022**, 34, 2201280.
6. C. Long, Y. Guan, C. Ren, J. Lu, C. Jin, P. Wang, P. Wang and H.-L. Xie, Near-infrared room temperature phosphorescence from single polymers containing benzoselenadiazole groups, *ACS Appl. Polym. Mater.* **2024**, 6, 4896-4903.
7. Q. Song, Z. Liu, J. Li, Y. Sun, Y. Ge and X.-Y. Dai, Achieving near-infrared phosphorescence supramolecular hydrogel based on amphiphilic bromonaphthalimide pyridinium hierarchical assembly. *Adv. Mater.* **2024**, 36, 2409983.
8. J. Tydlitát, M. Fecková, P. le Poul, O. Pytela, M. Klikar, J. Rodríguez-López, F. Robin-le Guen, S. Achelle, Influence of donor-substituents on triphenylamine chromophores bearing pyridine fragments. *Eur. J. Org. Chem.* **2019**, 9, 1921-1930.
9. X. Zhou, X. Bai, X. Zhang, J. Wu, Y. Liu. Cucurbit[8]uril induced molecular folding cascade assembly for NIR targeted cell imaging. *Adv. Optical Mater.* **2024**, 12, 2301550.
10. Z. Yang, W. Yin, S. Zhang, I. Shah, B. Zhang, S. Zhang, Z. Li, Z. Lei, H. Ma, Synthesis of AIE-active materials with their applications for antibacterial activity, specific imaging of mitochondrion



and image-guided photodynamic therapy. *ACS Appl. Bio Mater.* **2020**, 3, 1187-1196.